Molecular Biology of the Cell
Vol. 20, 2486–2494, May 1, 2009

Liver Progenitor Cells Fold Up a Cell Monolayer into a Double-layered Structure during Tubular Morphogenesis

Naoki Tanimizu,*† Atsushi Miyajima,† and Keith E. Mostov*

*Departments of Anatomy, and Biochemistry and Biophysics, University of California San Francisco, San Francisco, CA 94143-2140; and †Institute of Molecular and Cellular Biosciences, The University of Tokyo, Tokyo 113-0032, Japan

Submitted February 19, 2008; Revised February 27, 2009; Accepted March 3, 2009
Monitoring Editor: Asma Nusrat

Bile ducts are hepatic tubular structures that are lined by cholangiocytes, a type of liver epithelial cell. Cholangiocytes first form a single layer of cells, termed the ductal plate, surrounding the portal vein, which eventually remodels into the branching tubular network of bile ducts. The process of bile duct morphogenesis is not yet clear: a conventional model where cholangiocytes proliferate to duplicate a single layer of the ductal plate before lumen formation seems inconsistent with the observation that proliferation is dramatically reduced when hepatoblasts, liver progenitor cells, differentiate into cholangiocytes. Here, we developed a new culture system in which a liver progenitor cell line, HPPL, reorganizes from a monolayer to tubular structures in response to being overlaid with a gel containing type I collagen and Matrigel. We found that some of the HPPL in the monolayer depolarized and migrated to fold up the monolayer into a double-cell layer. These morphogenetic processes occurred without cell proliferation and required phosphatidylinositol 3-kinase and Akt activity. Later in morphogenesis, luminal space was generated between the two cell layers. This process, in particular enlargement of the apical lumen, involved transcriptional activity of HNF1β. Thus, using this sandwich culture system, we could segregate tubulogenesis of bile ducts into distinct steps and found that the PI3K/Akt pathway and HNF1β regulated different steps of the morphogenesis. Although the process of tubulogenesis in culture specifically resembled early bile duct formation, involvement of these two key players suggests that the sandwich culture might help us to find common principles of tubulogenesis in general.

INTRODUCTION

Tubules are an essential structural unit for numerous epithelial organs, such as lung, liver, and kidney. Epithelial tubes in different organs form by a wide variety of mechanisms (Hogan and Kolodziej, 2002; Lubarsky and Krasnow, 2003; Bryant and Mostov, 2008). Understanding the cellular and molecular basis of these mechanisms and discovering common principles that may underlie these diverse mechanisms is an important goal.

In the liver, bile ducts are tubular structures that consist of cholangiocytes, a type of liver epithelial cell. Bile ducts provide the excretory route for bile, which is synthesized by hepatocytes, another type of liver epithelial cell. Because bile is cytotoxic, abnormal development of bile ducts, which causes the accumulation of bile inside the liver, induces hepatic injury and ultimately results in severe liver fibrosis and cirrhosis (Schmucker *et al.*, 1990; Yoon and Gores, 2002; Paumgartner, 2006).

Cholangiocytes, the epithelial component of bile ducts, differentiate from liver progenitor cells called hepatoblasts around embryonic day 15 (E15) in mice (Lemaigre, 2003). Recent reports have identified the Notch and TGFβ signaling pathways and a transcription factor Hex, which regulate differentiation of cholangiocytes from hepatoblasts (McCright *et al.*, 2002; Kodama *et al.*, 2004; Tanimizu and Miyajima, 2004; Clotman *et al.*, 2005; Hunter *et al.*, 2007). After being induced, cholangiocytes acquire secretory functions and regulate the flow rate of bile and alkalinize it by secreting water and bicarbonate ion, respectively (Fitz, 2002). In parallel to this functional differentiation, cholangiocytes undergo tubular morphogenesis and develop the tubular tree of bile ducts.

Tubular morphogenesis of bile ducts has been studied by examining the structure of developing liver by histochemical techniques (Tan *et al.*, 1995). Cholangiocytes form a single-cell layer called the ductal plate around the portal vein; this ductal plate is then duplicated. Next, luminal space is generated between the two cholangiocyte layers. Finally, the ductal plate along with the luminal space is reorganized into tubules (Crawford, 2002). Recently, studies using mutant mice have identified several molecules necessary for tubular morphogenesis of bile ducts. In mice lacking HES1 (Kodama *et al.*, 2004) or lacking HNF1β specifically in the liver (Coffinier *et al.*, 2002), cholangiocytes differentiated from hepatoblasts but could not form bile duct tubules. Furthermore, abnormal formation of bile ducts that is generally recognized as "ductal plate malformation" has been reported in congenital human diseases such as Calori's disease and Meckel-Gruber syndrome (Low *et al.*, 2001). However, the precise mechanisms governing tubular morphogenesis of cholangiocytes have not been reported yet.

A major limitation in analyzing the mechanisms of intrahepatic bile duct formation has been a paucity of good cell culture models that recapitulate this process. To address these questions, we established an organotypic culture sys-

This article was published online ahead of print in *MBC in Press* (http://www.molbiolcell.org/cgi/doi/10.1091/mbc.E08–02–0177) on March 18, 2009.

Address correspondence to: Keith E. Mostov (keith.mostov@ucsf.edu).

tem in which liver progenitor cells form tubular structures. Considering that cholangiocytes make a single-cell layer of the ductal plate before tubular morphogenesis in vivo, we used a "sandwich" culture system. In this culture system, we cultured HPPL, a liver progenitor cell line, on the top of extracellular matrix (ECM) gel until they formed a monolayer and then placed another layer of gel over the monolayer. The top layer of gel induced the rearrangement of the monolayer into a double-cell layer and the generation of luminal space between the two cell layers. This novel culture system resembles development in vivo and has enabled us to address the mechanisms governing formation of bile duct tubules.

MATERIALS AND METHODS

Extracellular Matrix, Growth Factors, and Chemicals

Type I collagen was purchased from Cohesion Technologies (Palo Alto, CA). Growth factor reduced Matrigel and purified laminin-1 were from BD Biosciences (Bedford, MA). Mitomycin C (MMC) was from Sigma-Aldrich (St. Louis, MO). LY294002, a phosphatidylinositol 3-kinase (PI3K) inhibitor, and triciribine, an Akt inhibitor, were from Calbiochem (La Jolla, CA).

Cell Culture

HPPL were kept in DMEM/F12 (Sigma) containing 10% FBS (Invitrogen, Gaithersburg, MD), 1× insulin/transferrin/selenium (ITS; Invitrogen), 10 mM nicotinamide (Wako, Osaka, Japan), 0.1 μM dexamethasone (Dex; Sigma), 5 mM L-glutamine, 5 ng/ml hepatocyte growth factor (HGF; gift of the late Ralph Schwall, Genentech) and epidermal growth factor (EGF; Invitrogen, Carlsbad, CA). To prepare the bottom layer of culture, 1 volume of Matrigel were mixed with 4 volumes of type I collagen and 150 μl of the gel were added to each 1-cm diameter tissue culture insert (0.02-μm Anopore Membrane; Millipore, Billerica, MA). HPPL were plated on the bottom layer at a density of 1×10^5 cells. After 2 d of incubation, the monolayer of HPPL was overlaid with another layer of ECM gel. After incubation at 37°C for 2 h to solidify the gel, 500 μl of DMEM/F12 containing EGF and HGF were added to the top of the gel and under the culture insert.

To block proliferation, HPPL were incubated in the presence of 0.5 or 1 μg/ml MMC for 6 h before the overlay. To inhibit the activity of PI3K or Akt, HPPL were overlaid with ECM gel and then incubated in the presence of 20 μM LY294002 or 2 μM triciribine.

Immunofluorescence Microscopy

Mouse embryonic and neonatal livers were embedded in OCT compound and frozen. These were used for preparation of thin sections by using a cryostat (Leica, St. Gallen, Switzerland). Sections were incubated in PBS containing 4% paraformaldehyde (PFA) at 4°C for 10 min. Samples of sandwich culture were treated with collagenase and fixed in PFA solution as previously reported (O'Brien *et al.*, 2006). Primary antibodies used in this study were rabbit anti-cytokeratin 19 (CK19; 1:2000; Tanimizu *et al.*, 2003), rat anti-ZO1 (1:2000; a gift from Dr. Bruce Stevenson, University of Alberta), rat anti-Ki67 (1:200; Dako, Carpinteria, CA), rat anti-EpCAM (1:500; BD Biosciences), rabbit anti-Akt (1:100; Cell Signaling Technology, Danvers, MA), and rabbit anti-phospho-Thr308 Akt (1:100; Cell Signaling Technology) antibodies. Signals were visualized with AlexaFluor conjugated secondary antibodies (Molecular Probes, Eugene, OR) used at a dilution of 1:500. F-actin bundles were detected with AlexaFluor 488– or 546–conjugated phalloidin (Molecular Probes) at a dilution of 1:250. Nuclei were counterstained with Hoechst 34580. Samples were examined on Zeiss LSM 510 and Olympus FV1000D IX81 confocal laser scanning fluorescence microscopes (Thornwood and Melville, NY, respectively).

Overexpression of a Dominant Negative Form of HNF1β

The sequences of HNF1β263fsinGG (dominant negative HNF1β: dnHNF1β) were amplified from the first-strand cDNA derived from HPPL by using following primers: 5′-GCC ACC ATG GTG TCC AAG CTC ACG TCG C-3′ and 5′-GCG GCC GCC TAA CCG GCC TCC CTC TCT TCC TTG-3′. PCR products were inserted into pCRII vector (Invitrogen). After verifying the sequence, the fragment of dnHNF1β was transferred into EcoRI-NotI sites of pMXs-IRES-GFP. pMXs-dnHNF1β-IRES-GFP was introduced into BOSC23, a virus-packaging cell. Packaged virus collected from 10 ml of culture medium by centrifugation was resuspended in 2 ml of fresh medium. After incubating HPPL with virus solution for 2 d, infection efficiency was checked on a FACScalibur (BD Biosciences, San Diego, CA) by examining expression of green fluorescent protein (GFP).

Live Cell Imaging

HPPL expressing GFP were generated as described above. For imaging under a microscope, we used 24-well glass bottom dishes instead of culture inserts in order to permit focusing on cells in the culture. We selected four areas in a well and took ~16 X-Y images at different planes along the Z-axis using Olympus FV1000D IX81 confocal microscope. At 2 h after the overlay, we started taking images every 40 min for 24 h. Our system includes an Olympus ZDC system that ensures the constant distance between an objective lens and the bottom of the dish during imaging.

RESULTS

HPPL Form a Tubular Network in Sandwich Culture

Histochemical data indicate that cholangiocytes, which differentiate from hepatoblasts around the portal vein, form the single-cell layer of the ductal plate before starting tubular morphogenesis. The ductal plate is reorganized into bile duct tubules later in perinatal liver (Crawford, 2002). To mimic a process of tubular morphogenesis that starts from a single layer of cells, we overlaid ECM gel on top of a monolayer of liver progenitor cells. A similar protocol has been used with Madin-Darby canine kidney (MDCK) cells to induce tubular structures: MDCK cells generate a tubular network from a monolayer after overlaying with collagen gel (Hall *et al.*, 1982; Ojakian and Schwimmer, 1994; Zuk and Matlin, 1996; Ojakian *et al.*, 2001). For optimizing culture condition, we used HPPL, a liver progenitor cell line that differentiates into both hepatocytes and cholangiocytes in vitro (Tanimizu *et al.*, 2004). We first cultured HPPL on a culture insert coated with laminin until they formed a confluent monolayer, and then we covered the monolayer with either type I collagen gel or a mixture of type I collagen gel and Matrigel. However, HPPL did not form tubular structures under either condition. We then cultured HPPL on an ECM gel that was pure type I collagen gel, collagen gel containing 10, 20, 30, 40, or 60% Matrigel, or pure Matrigel. HPPL formed a monolayer on collagen gel containing 10 or 20% Matrigel. Therefore, we covered the monolayer on 20% Matrigel with a mixture of collagen and Matrigel that had the same composition as the bottom layer (Figure 1A). We called this system "sandwich culture."

Two days after the overlay, we visualized F-actin localization by incubating with AlexaFluor 488–conjugated phalloidin. We observed that HPPL formed areas surrounded by thick F-actin bundles (Figure 1B), suggesting that HPPL formed a tubular network where luminal space was surrounded by polarized cells. To better visualize the luminal space, we reconstructed images of confocal vertical (X-Z) sections after staining with anti-cytokeratin 19 (CK19), a cholangiocyte marker, F-actin, and ZO1 showing that HPPL expressed CK19 and localized ZO1 at the apical tip of the lateral domain surrounding the apical luminal space (Figure 1C). Thus, we considered that HPPL reorganized a monolayer into tubular structures in sandwich cultures.

Proliferation Is Not Necessary for Tubular Morphogenesis In Vitro

To test whether proliferation of HPPL is necessary for tubular morphogenesis, we blocked proliferation of HPPL by adding MMC, a DNA synthesis inhibitor, to the culture 6 h before the overlay. At 2 d after overlay, we estimated the area of the tubular structures by using NIH ImageJ (http://rsb.info.nih.gov/ij/) to measure the area surrounded by thick actin bundles in confocal images. We found that MMC did not reduce the area of tubular structures (Figure 2, A and B), indicating that proliferation is not a crucial event for HPPL to undergo tubular morphogenesis in sandwich culture. MMC inhibited proliferation of HPPL in a separate,

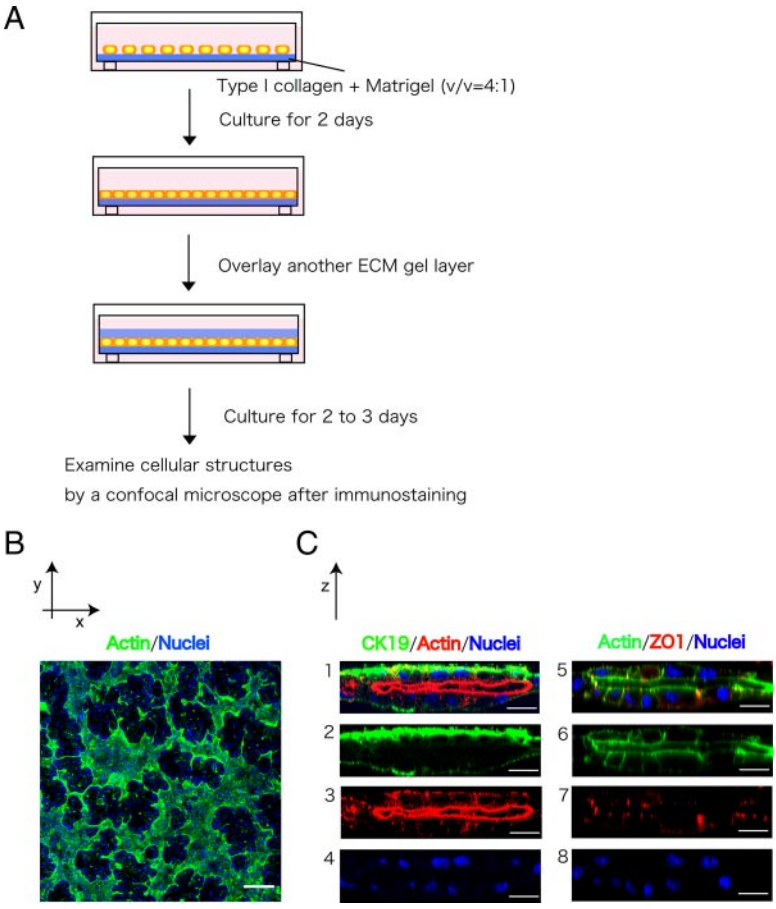

Figure 1. HPPL form tubular structures in sandwich culture. (A) Schematic view of sandwich culture. HPPL were plated on gel containing type I collagen and Matrigel. After HPPL form a monolayer during 2 d of incubation, another layer of gel was overlaid on the monolayer. After additional 2 or 3 d of incubation, cells were fixed and examined with a confocal microscope after immunostaining. (B) A low-magnification image of sandwich culture stained with AlexaFluor 488–conjugated phalloidin and Hoechst34580. A tubular network was visualized as the area surrounded by thick F-actin bundles. Scale bar, 100 μm. (C) Vertical sections of sandwich culture. Cultures were stained with anti-cytokeratin 19 (CK19) antibodies and phalloidin (1–4) or phalloidin and anti-ZO1 antibodies (5–8). CK19$^+$ cells formed the apical lumen surrounded by F-actin bundles. Formation of tight junction was visualized with ZO1 staining. Scale bars, 20 μm.

nonsandwich culture, indicating that the drug worked (Supplementary Figure S1).

Cholangiocytes Do Not Significantly Proliferate during Tubular Morphogenesis In Vivo

Next, we wanted to test whether cholangiocytes in vivo form bile ducts with or without proliferation. To examine the proliferation of cholangiocytes undergoing tubular morphogenesis, we stained frozen sections of E18, postnatal day 0 (P0) and P8 livers with antibodies against CK19 and Ki67, a marker for cells in G1, S, or G2/M phases. In E18 liver, most CK19$^+$ cholangiocytes were negative for Ki67, whereas other liver cells including hepatocytes were positive for Ki67 (Figure 2C). Similarly, in P0 liver, CK19$^+$ cholangiocytes

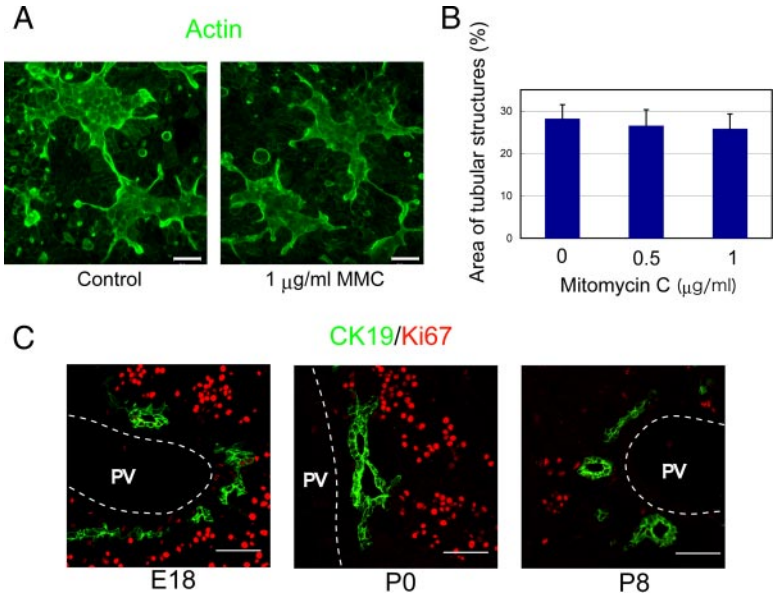

Figure 2. Proliferation is not a crucial event for tubular morphogenesis in vitro and in vivo. (A) Low-magnification images at 2 d after the overlay show tubular structures surrounded by thick F-actin bundles with or without mitomycin C (MMC). MMC, a DNA synthesis inhibitor, was added to culture for 6 h before the overlay. Scale bars, 50 μm. (B) The area of tubular structures in culture was statistically unchanged with or without MMC. The experiment was independently repeated four times. Four fields were selected from each culture and the area of tubular structures in a field was measured using NIH ImageJ after staining with AlexaFluor 488–conjugated phalloidin. (C) Expression of Ki67 in cholangiocytes during bile duct morphogenesis. Frozen sections of embryonic day 18 (E18), postnatal day 0 (P0), and P8 livers were stained with anti-CK19 and anti-Ki67 antibodies. Cells in the parenchyma including hepatocytes were mostly positive for Ki67 in E18 and P0 livers, whereas CK19$^+$ cholangiocytes were mostly negative for Ki67. PV, portal vein. Scale bars, 50 μm.

were negative for Ki67, whereas other cells were still positive for Ki67 (Figure 2C). In P8 liver, both $CK19^+$ cholangiocytes and $CK19^-$ hepatocytes became mostly negative for Ki67 (Figure 2C). These data suggested that cholangiocytes form the tubular structures of bile ducts without significant proliferation in vivo. Thus, we further examined the sandwich culture, where tubular structures were formed without significant proliferation, in order to understand how the monolayer of the ductal plate turns to bile duct tubules.

Tubules Form In Vitro by Cell Migration and Rearrangement

To analyze the process of tubular morphogenesis, we took images of cultures at different time points after the overlay and examined the localization of F-actin bundles and nuclei. See Figure 3A, 1–7: 1, HPPL localized F-actin bundles around the cell cortex in a monolayer; 2, a number of cells lost the apical F-actin bundles (arrowheads), suggesting a loss of apico-basal polarity at 6 h after the overlay; 3, the nucleus of a depolarized cell (an arrowhead) was positioned differently compared with polarized cells, indicating depolarized cells moved up along the Z-axis about 16 h after the overlay; 4 and 5, the number of cells on top of the bottom cell layer increased between 20 and 32 h after the overlay (arrowheads); and 6 and 7, after the second cell layer almost covered the bottom cell layer, the apical luminal space was evident at 48 h and then expanded.

To characterize dynamic stages of morphogenesis with higher spatio-temporal resolution, we further examined the localization of F-actin bundles and β-catenin between 14 and 23 h after the overlay (reconstructed vertical X-Z sections are shown in Figure 3B, 1–10; X-Y sections through the top and bottom of the cell layer are shown in Supplementary Figure S2, A–E). The right side of panels is the edge of the tubular area (panel 1 of Supplementary Figure S2, A–E). Cells in the second layer were first observed only in the right side (panels 1 and 6, closed arrowheads) and then also in the center (panels 2–4 and 7–9, closed arrowheads) and eventually reached to the left side of the image (panels 5 and 10), indicating that cells migrated from the edge to the center of the tubular area. Interestingly, cell–cell contacts shown by β-catenin staining were clear in the bottom cell layer (open arrowheads in panel 6) throughout these time points, but ere less clear between cells in the second layer (an open arrow in panel 6). At 23 h, β-catenin was occasionally observed at cell–cell contact between cells in the second layer (open arrowhead in panel 10). The change of β-catenin localization suggests that intercellular junctions were partly lost during

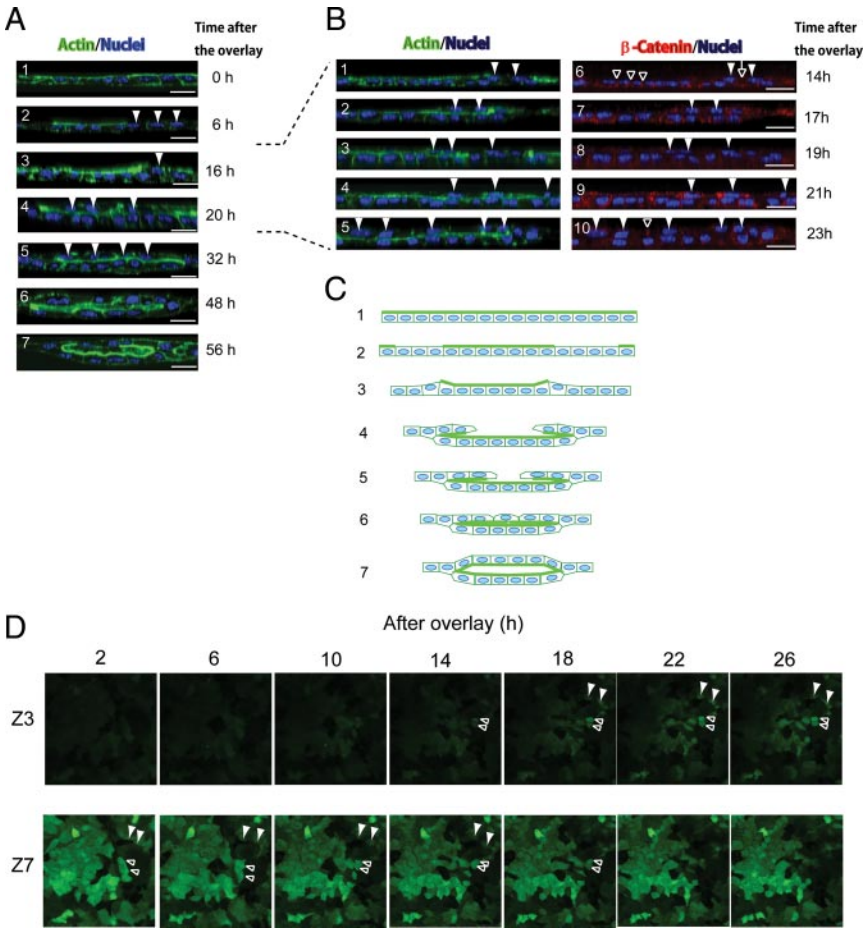

Figure 3. A monolayer of HPPL folds up into tubular structures in sandwich culture. (A) Time course of tubular morphogenesis after the overlay. The overlay of ECM gel on a monolayer of HPPL induced exclusion of F-actin bundles from the apical domain, indicating depolarization of cells (arrowheads in panel 2). Panels 3–5 suggest that depolarized cells first migrated along the Z-axis (an arrowhead in panel 3) and then back along the bottom cell layer (arrowheads in panels 4 and 5). Finally, the apical luminal space was evident at 48 h after the overlay (panel 6) and then expanded (panel 7). X-Y images were taken every 0.7 μm along the Z-axis at each time point using a LSM510 confocal laser scanning microscope and images of a vertical (X-Z) section was reconstructed by using Zeiss LSM software. Scale bars, 20 μm. (B) Time course between 14 and 23 h after the overlay. Cells in the second layer (arrowheads) appeared in the right side of the image (panels 1 and 6) and then were observed also in the center of images (panels 2–4 and 7–9), and eventually reached to the left side (panels 5 and 10). β-Catenin localization at cell–cell contacts were clear between cells in the bottom layer (open arrowheads in panel 6) but not between cells in the second layer (an open arrow in panel 6). Later, β-catenin reappeared at cell–cell contact at 23 h (an open arrowhead in panel 10). X-Y images were taken every 0.5 μm along the Z-axis at each time point using an Olympus FV1000D IX81 confocal laser scanning microscope and images of a vertical (X-Z) section was reconstructed by using Olympus viewer software. Scale bars, 20 μm. (C) On the basis of images at different time points, we propose a model of in vitro tubular morphogenesis in which a monolayer of HPPL folds up into tubular structures. Thick green lines represent F-actin bundles. (D) X-Y images of time-lapse movies between 2 and 26 h after the overlay. HPPL were labeled with GFP. Images at 16 different X-Y planes along the Z-axis were taken in a selected area every 40 min using an Olympus FV1000D IX81 confocal microscope. Panels of the Z7 series show X-Y images of the original monolayer, whereas panels of the Z3 series show a X-Y plane above the monolayer where no cells were initially observed. As indicated by open and closed arrowheads, some cells disappeared from the Z7 plane and instead appeared in the Z3 plane, indicating these cells moved up along the Z-axis.

migration and then were reconstituted around the time when formation of the second layer was almost completed. On the basis of these data, we proposed a model that a monolayer of HPPL folds up into tubular structures (Figure 3C). In this model, depolarized HPPL migrate on a cluster of cells that maintain apico-basal polarity and enclose a volume that eventually becomes the apical luminal space.

The morphogenesis in the model proposed in Figure 3C depends on cell motility. To confirm cellular movement during morphogenesis, we introduced GFP into HPPL to visualize live cells and followed the culture under a confocal microscope. At 2 h after the overlay, we started taking X-Y images at 16 planes along the Z-axis at multiple areas every 40 min. We present movies at the third and seventh X-Y planes, which are, respectively, named Z3 and Z7 planes, of a representative area (Supplementary Movies) and display selected X-Y images from the movies (Figure 3D). HPPL in the original monolayer were followed in the movie of the Z7 plane and panels of selected times from the Z7 series, whereas the area above the monolayer was followed in the movie of the Z3 plane and panels of the Z3 series. As indicated by open and closed arrowheads in Figure 3D, some cells disappeared from the Z7 plane and instead could be observed correspondingly appearing in the Z3 plane. These cellular movements similarly could be observed in the movies of the Z3 and Z7 planes. These data indicate that some of HPPL migrated along the Z-axis during morphogenesis and further support the model shown in Figure 3C.

The PI3K/Akt Pathway Is Essential for Tubular Morphogenesis

We went on to use the sandwich culture system to address the involvement of several important signaling systems in bile duct morphogenesis. It has been shown that PI3K defines the leading edge of cells during migration and the basal domain of epithelial cells during apico-basal polarization (Weiner *et al.*, 2002; Gassama-Diagne *et al.*, 2006; Martin-Belmonte *et al.*, 2007) by producing phosphatidyl-inositide-3,4,5-triphosphate. To test whether the PI3K pathway regulates tubular morphogenesis of HPPL, we first added LY294002, an inhibitor for PI3K, to sandwich cultures at the time of overlay. We found that 20 μM of LY294002 significantly reduced the area of tubular structures (Figure 4A). A similar effect was observed by using wortmannin, another

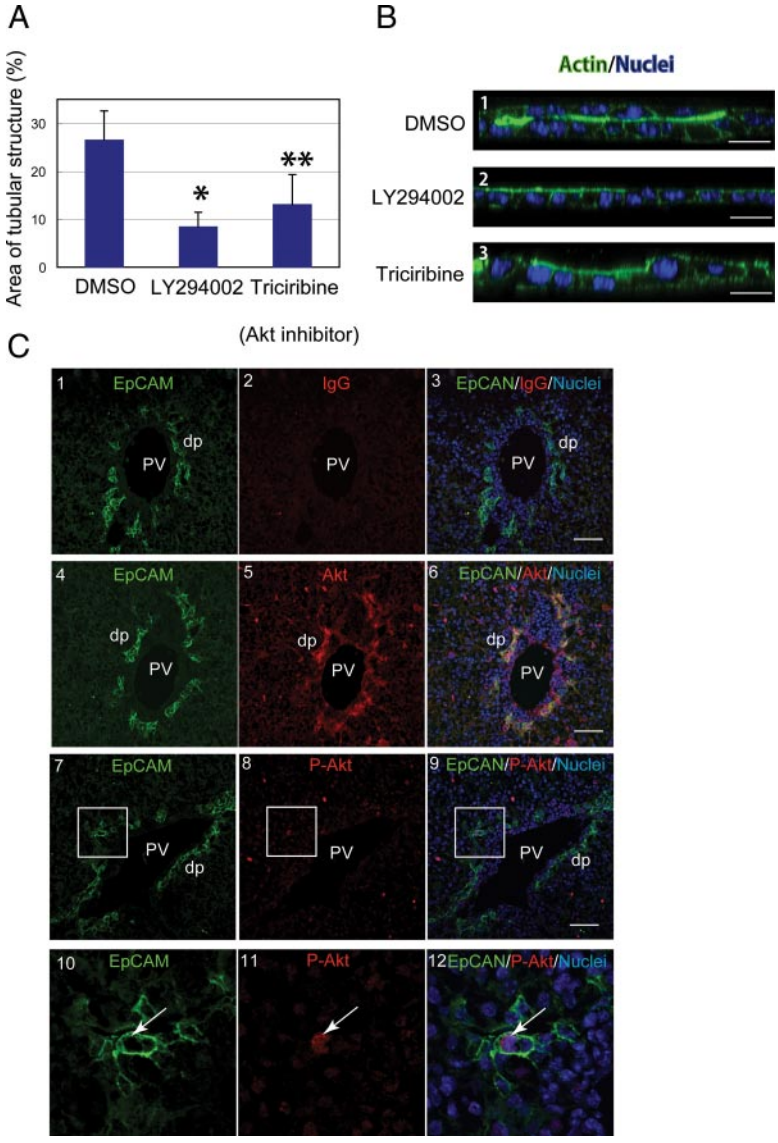

Figure 4. The process of a monolayer of HPPL folding up into tubular structures is regulated by the PI3K/Akt pathway. (A) LY294002, a PI3K inhibitor, or triciribine, an Akt inhibitor, were added to cultures at the time of the overlay. The area of tubular structures was significantly reduced in the presence of LY294002 or triciribine. The culture was independently repeated four times. Four fields were selected from each culture, and areas surrounded by thick F-actin bundles in a field were measured using NIH ImageJ after staining with AlexaFluor 488–conjugated phalloidin. *p $<$0.01 and **p $<$0.05, respectively. (B) HPPL formed two cell layers in the control culture at 2 d after the overlay. On the other hand, HPPL remained as a monolayer in the presence of either LY294002 or triciribine. Scale bars, 20 μm. (C) Sections of E18 liver were stained with anti-EpCAM and anti-Akt (panels 4–6) or anti-phospho-Thr308 Akt antibodies (panels 7–12). Boxes in panels 7~9 are enlarged in panels 10–12. As a negative control for Akt and phosho-Thr308 Akt staining, rabbit IgG was used (panels 1–3). Cholangiocytes forming ductal plates (dp) express both EpCAM and Akt (panels 4–6). Furthermore, we found cholangiocytes positive for both EpCAM and phospho-Thr308 Akt (arrows in panels 10–12). PV, portal vein. Scale bars, 50 μm.

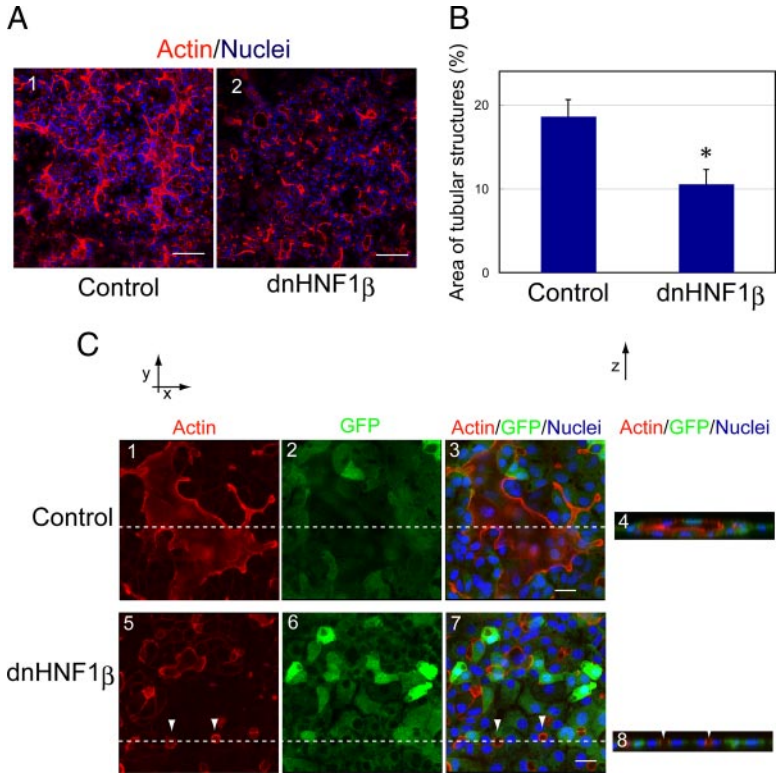

Figure 5. Dominant negative HNF1β inhibits tubular morphogenesis of HPPL. (A) Images at 2 d after the overlay show that tubular structures surrounded by F-actin bundles were observed in the control culture but not in dnHNF1β culture. Scale bars, 100 μm. (B) The area of tubular structures was significantly reduced by overexpression of dnHNF1β. *$p < 0.01$. (C) A large area surrounded by F-actin bundle was observed in a field of the control culture. The X-Z section (panel 4) along the lines in panels 1–3 showed an apical luminal space in the control culture. On the other hand, only tiny areas surrounded by F-actin bundles (arrowheads) were observed in culture overexpressing dnHNF1β (panels 5–8). Retrovirus vector pMXs-dnHNF1β-IRES-GFP was used to express dnHNF1β in HPPL, whereas pMXs-IRES-GFP was used as the control. Scale bars, 20 μm.

PI3K inhibitor (data not shown). Next, we tested whether Akt, a kinase downstream of PI3K, is involved in tubular morphogenesis of HPPL by adding triciribine, an Akt inhibitor. We found that 2 μM of triciribine (a concentration where it is specific for Akt) significantly reduced tubular structures in culture (Figure 4A). Vertical sections of cultures at 48 h after overlay demonstrated that HPPL remained as a monolayer in the presence of LY294002 or triciribine (Figure 4B-2 and 3) whereas HPPL formed a double-cell layer in the control (Figure 4B1). (With triciribine, there was a small amount of upward movement of some nuclei, whereas no such movement was seen with LY294002. The significance of this difference is not clear, but might suggest that Akt is only one of several pathways downstream of PI3K involved in tubular morphogenesis.) These data indicated that the PI3K/Akt pathway is necessary for tubular morphogenesis of HPPL.

To know whether the PI3K/Akt pathway is involved in bile duct morphogenesis in vivo, we prepared sections of E18 liver and examined expression of Akt and phosphorylated Akt in cholangiocytes. We found that Akt was expressed in the periportal area including ductal plates (Figure 4C, 4–6). In addition, we detected signals for phospho-Thr308 Akt on E18 liver sections (Figure 4C, 7–9) and found cholangiocytes positive for phospho-Thr308 Akt (arrows in Figure 4C, 10–12). These data suggest that the PI3K/Akt pathway might be also important for bile duct morphogenesis in vivo.

HNF1β Is Involved in Forming Tubular Structures In Vitro

HNF1β is a transcription factor that is expressed in many tubular structures including bile ducts (Coffinier *et al.*, 1999). Because liver-specific depletion of HNF1β resulted in abnormal formation of intrahepatic bile ducts (Coffinier *et al.*, 2002), HNF1β has been thought to regulate bile duct morphogenesis. To test whether HNF1β regulates tubular morphogenesis of HPPL, we overexpressed HNF1β263fsinGG, a dominant negative form of HNF1β (dnHNF1β; Bai *et al.*, 2002), by using a retrovirus vector, pMXs-dnHNF1β-IRES-GFP. GFP expression indicated that infection efficiency was more than 80%. We compared the area of tubular structures in culture overexpressing dnHNF1β with the control (Figure 5A) and found that dnHNF1β significantly inhibited tubular morphogenesis of HPPL (Figure 5B). We observed normal luminal spaces in the control culture (Figure 5C, 1–4), whereas tiny luminal spaces were observed in cultures overexpressing dnHNF1β (arrowheads in Figure 5B, 5–8). These results indicated that activity of HNF1β is involved in HPPL tubulogenesis in vitro, most likely in enlargement of lumens.

DISCUSSION

We have established a novel organotypic culture system in which HPPL, a mouse liver progenitor cell line, form tubular structures. Using this system, we have demonstrated that depolarized HPPL migrate back along the monolayer, "folding up" to make a double-cell layer. The evidence is that in vertical sections of cultures, F-actin bundles disappeared from the apical domain in a number of cells, and then these depolarized cells were observed on the original cell layer, which eventually formed the second cell layer. After completing formation of the double-cell layer, HPPL generated the apical luminal space between two cell layers.

We recently reported that HPPL embedded as single cells in three-dimensional (3D) ECM gel formed spherical cysts. These cells developed cholangiocyte-type epithelial polarity and acquired secretory functions (Tanimizu *et al.*, 2007). On the other hand, in the present report we observed formation of a tubular network in sandwich culture, where HPPL rearrange the monolayer into tubular structures. These cells

have not fully acquired secretory functions (Supplementary Figure S3). Thus, we consider that we could examine the correlation between epithelial polarization and functional differentiation (secretory function) of liver progenitor cells along the cholangiocyte lineage in 3D cyst culture, whereas we could analyze the process of tubular morphogenesis of bile ducts in sandwich culture. By combining the two approaches we will be able to understand the molecular mechanisms governing bile duct morphogenesis. Recently, Hashimoto *et al.* (2008) reported mature cholangiocytes isolated from adult rat formed tubular structures in collagen overlay culture. They showed transport of fluorescein diacetate into the apical luminal space, which we could not observe. Those authors did not, however, examine the mechanisms of cell movement or signaling pathways involved in tubular morphogenesis. A further advantage of our system is that we used liver progenitor cells rather than mature cholangiocytes and therefore, we could more directly study the developmental process of bile duct formation.

Bile duct morphogenesis in vivo can be divided into three distinct stages: formation of a double-cell layer, generation of the apical luminal space, and reorganization of the ductal plate along with the luminal space into tubules. Our results that a monolayer of HPPL folds up into a tubular structure have demonstrated a possible pathway of bile duct morphogenesis, in particular a potential mechanism for the first step. At least three major types of nonmutually exclusive models can be envisioned as to how the initial monolayer of cells in a ductal plate can be converted to a double layer of cells in vivo (Figure 6). In model 1, cells in the monolayer of the plate divide, forming a second layer. In model 2, certain hepatoblasts in the adjacent parenchyma differentiate into cholangiocytes and form the second layer of the plate. In model 3, which best fits the morphogenesis of HPPL in sandwich culture, some cells in the initial monolayer rearrange themselves by moving on top of the original monolayer, thereby forming the second layer.

Model 1 relies on proliferation of cells in the ductal plate to form the double layer. However, as we observed that proliferation is dramatically reduced when hepatoblasts differentiate to cholangiocytes, duplication of a single-cell layer by proliferation is not likely to be a major process in generating a double-cell layer in vivo. On the other hand, models 2 and 3, respectively, rely on recruitment of cells from outside the monolayer and migration of cells in the ductal plate to form the double layer. Thus, in both cases, proliferation of hepatoblasts is not necessary to form the second layer and these models of in vivo bile duct morphogenesis seem more likely compared with model 1.

In model 2, certain hepatoblasts next to the first layer of cholangiocytes differentiate to cholangiocytes, which form the second layer of the ductal plate. In support of this model, recent reports indicate that activin/TGFβ signaling is activated more strongly in hepatoblasts near the portal vein than those in the parenchyma of fetal liver and thereby induces cholangiocyte differentiation of hepatoblasts only near the portal vein (Clotman *et al.*, 2005). In the model where cholangiocyte differentiation is induced outside of the first layer of the ductal plate, the activin/TGFβ signaling pathway may be preferable to the Notch signaling pathway, which also induces cholangiocytes from hepatoblasts (McCright *et al.*, 2002; Tanimizu and Miyajima, 2004). In contrast

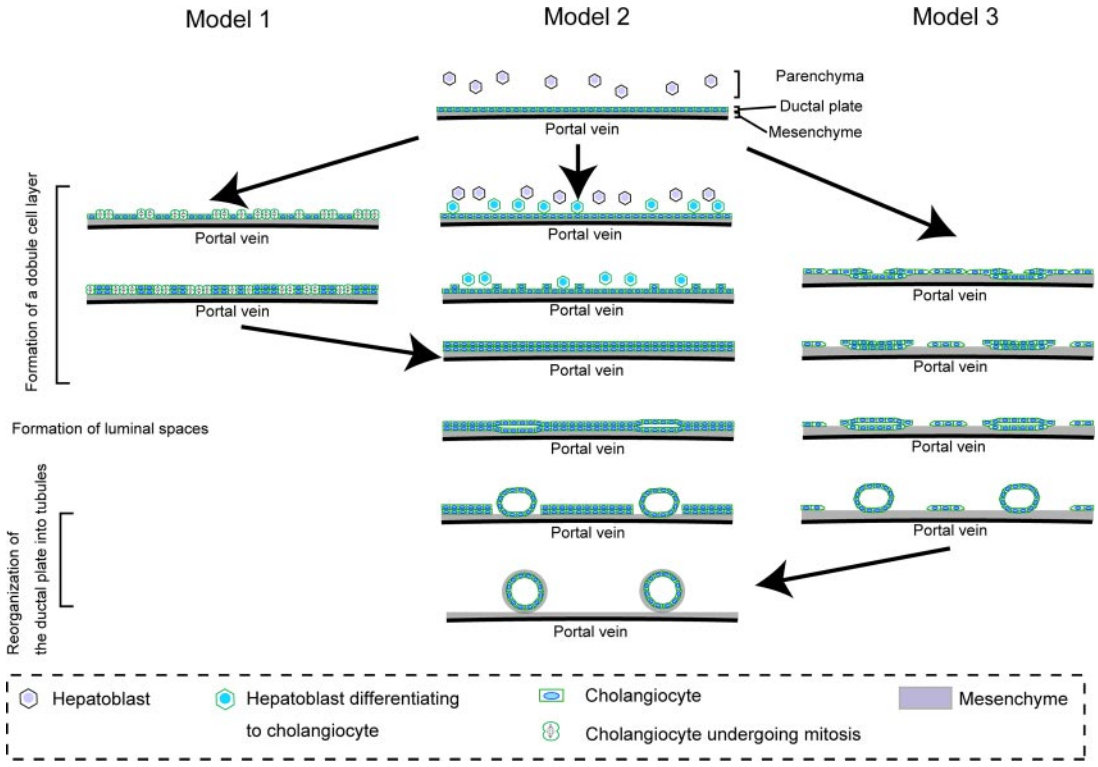

Figure 6. Three possible models for bile duct morphogenesis. Bile duct morphogenesis starts from a single layer of cholangiocyte called the ductal plate around the portal vein. To form a double-cell layer, we considered three possible models. Cholangiocytes proliferate to generate the second layer of the ductal plate (model 1), hepatoblasts outside the first layer are induced to differentiate to cholangiocytes (model 2), or cholangiocytes fold up to form a double layer (model 3). After luminal space is generated between the two cell layers, the ductal plate is reorganized into tubular structures. During this stage, small, flat luminal spaces are enlarged and become round. Cholangiocytes that remain in the ductal plate eventually disappear.

to the Notch pathway, which requires direct interaction between Jagged1$^+$ periportal cells and Notch2$^+$ hepatoblasts to induce cholangiocyte differentiation of hepatoblasts, the activin/TGFβ signal can be activated without direct cell–cell interaction.

During tubular morphogenesis in some types of epithelial structures, such as mammary acini, cell death is important for creation of the luminal space (Debnath and Brugge, 2005). In the case of bile duct morphogenesis, apoptotic cell death might be an important event during rearrangement of the ductal plate (Terada and Nakanuma, 1995; Sergi *et al.*, 2000). Given that each portal vein is usually associated with one or two bile ducts, only part of the cholangiocytes that form the ductal plate develop into tubular structures. Other cholangiocytes that remain in the ductal plate gradually regress. If bile duct morphogenesis proceeds via model 1 or 2, a significant number of cells would remain in the ductal plate, which would be eliminated later. However, apoptotic cholangiocytes were not frequently observed in mouse liver at E18, P5, and P10 (Supplementary Figure S4). In contrast, many cells would be predicted to leave the ductal plate to form the second layer during tubulogenesis, and fewer cells need to be eliminated by apoptosis, if morphogenesis proceeds via model 3.

In our sandwich culture, no pool of progenitor cells that could differentiate to cholangiocytes and be recruited to form a second layer was present, yet a second layer was formed. This indicates that it is at least possible for double layer to form without recruitment of outside cells. In addition, the result that cholangiocytes do not frequently die by apoptosis (Supplementary Figure S4) is consistent with model 3. On the other hand, the previously reported in vivo evidence that activin/TGFβ signaling involved in bile duct development is supportive of model 2. Thus, although model 1 seems unlikely in light of our data, we cannot determine whether model 2 or 3 are better able to explain bile duct morphogenesis in vivo. It is of course possible that both models 2 and 3 may occur during bile duct development in vivo.

The process of folding up a monolayer can be segregated into three steps: the first step is loss of apico-basal polarity, the second is migration of depolarized cells, and the third is expansion of the apical luminal space. Morphogenesis was completely blocked by inhibiting PI3K. So far, we cannot tell whether PI3K is only necessary for the first step or also needed for later steps. However, because Akt was constitutively phosphorylated during the process of folding up (data not shown), it is tempting to speculate the PI3K/Akt pathway is involved in all three steps. Morphogenesis was also decreased by reducing the activity of HNF1β, though the nature of the effect was quite different from blocking the PI3K/Akt pathway. In cultures with dnHNF1β, F-actin in the apical domain disappeared and only much smaller lumens were observed. (In contrast, apical F-actin remained in cultures with LY294002 and triciribine.) This suggests that transcriptional activity of HNF1β is necessary for HPPL to expand the apical luminal space, but not to undergo the initial event where they depolarize before starting migration. This illustrates how different molecular pathways are involved in distinct steps in tubulogenesis.

In vivo, folding of a monolayer to produce a tube has been described during formation of the neural tube (Zohn *et al.*, 2003). In this case, a single lumen is produced. In contrast during formation of bile ducts, multiple lumens are generated and these rearrange to eventually produce a branching tubular network of bile ducts. As far as we know, this type of process does not occur normally during development of other epithelial organs, e.g., kidney or lung. Even though tubular morphogenesis in different organs utilizes apparently distinct mechanisms, many of the same molecules such as PI3K/Akt and HNF1β have been implicated in formation of a variety of tubular structures (Coffinier *et al.*, 2002; Tang *et al.*, 2002; Liu *et al.*, 2004; Lebrun *et al.*, 2005; Kim and Dressler, 2007). This suggests that there may be common principles of tubulogenesis that underlie seemingly diverse mechanisms of tubulogenesis. Using in vitro organotypic culture systems, we can access molecular mechanisms of morphogenetic processes in detail help us to find out common principles of tubular morphogenesis during organogenesis (Ojakian *et al.*, 2001; Yu *et al.*, 2003; Zegers *et al.*, 2003; Walid *et al.*, 2008).

In summary, using our newly developed sandwich culture system, we found that HPPL folds a monolayer up to make a double-cell layer and then form tubular structures. This is an unusual (possibly unique) and interesting variation on known mechanisms for tubule formation in various organs. In addition, because tubulogenesis in the culture seems very similar to in vivo bile duct morphogenesis, our sandwich culture system of liver progenitor cells is likely to prove useful in understanding abnormal bile duct morphogenetic processes such as ductal plate malformation.

ACKNOWLEDGMENTS

We thank the members of the Mostov and Miyajima laboratories for helpful discussions. N.T. was supported by a Pilot/Feasibility funding from the Liver Center of University of California San Francisco. This work was supported by grants from the National Institutes of Health to K.E.M. and by a research grant from the Ministry of Education, Sports, Science, and Technology, Japan, to N.T.

REFERENCES

Bai, Y., Pontoglio, M., Hiesberger, T., Sinclair, A. M., and Igarashi, P. (2002). Regulation of kidney-specific Ksp-cadherin gene promoter by hepatocyte nuclear factor-1beta. Am. J. Physiol. Renal. Physiol. *283*, F839–F851.

Bryant, D. M., and Mostov, K. E. (2008). From cells to organs: building polarized tissue. Nat. Rev. Mol. Cell Biol. *9*, 887–901.

Clotman, F., Jacquemin, P., Plumb-Rudewiez, N., Pierreux, C. E., Van der Smissen, P., Dietz, H. C., Courtoy, P. J., Rousseau, G. G., and Lemaigre, F. P. (2005). Control of liver cell fate decision by a gradient of TGF beta signaling modulated by Onecut transcription factors. Genes Dev. *19*, 1849–1854.

Coffinier, C., Barra, J., Babinet, C., and Yaniv, M. (1999). Expression of the vHNF1/HNF1beta homeoprotein gene during mouse organogenesis. Mech. Dev. *89*, 211–213.

Coffinier, C., Gresh, L., Fiette, L., Tronche, F., Schutz, G., Babinet, C., Pontoglio, M., Yaniv, M., and Barra, J. (2002). Bile system morphogenesis defects and liver dysfunction upon targeted deletion of HNF1beta. Development *129*, 1829–1838.

Crawford, J. M. (2002). Development of the intrahepatic biliary tree. Semin. Liver Dis. *22*, 213–226.

Debnath, J., and Brugge, J. S. (2005). Modelling glandular epithelial cancers in three-dimensional cultures. Nature Rev. *5*, 675–688.

Fitz, J. G. (2002). Regulation of cholangiocyte secretion. Semin. Liver Dis. *22*, 241–249.

Gassama-Diagne, A., Yu, W., ter Beest, M., Martin-Belmonte, F., Kierbel, A., Engel, J., and Mostov, K. (2006). Phosphatidylinositol-3,4,5-trisphosphate regulates the formation of the basolateral plasma membrane in epithelial cells. Nat. Cell Biol. *8*, 963–970.

Hall, H. G., Farson, D. A., and Bissell, M. J. (1982). Lumen formation by epithelial cell lines in response to collagen overlay: a morphogenetic model in culture. Proc. Natl. Acad. Sci. USA *79*, 4672–4676.

Hashimoto, W., Sudo, R., Fukasawa, K., Ikeda, M., Mitaka, T., and Tanishita, K. (2008). Ductular network formation by rat biliary epithelial cells in the dynamical culture with collagen gel and dimethylsulfoxide stimulation. American J. Pathol. *173*, 494–506.

Hogan, B. L., and Kolodziej, P. A. (2002). Organogenesis: molecular mechanisms of tubulogenesis. Nat. Rev. Genet. *3*, 513–523.

Hunter, M. P., Wilson, C. M., Jiang, X., Cong, R., Vasavada, H., Kaestner, K. H., and Bogue, C. W. (2007). The homeobox gene Hhex is essential for proper hepatoblast differentiation and bile duct morphogenesis. Dev. Biol. *308*, 355–367.

Kim, D., and Dressler, G. R. (2007). PTEN modulates GDNF/RET mediated chemotaxis and branching morphogenesis in the developing kidney. Dev. Biol. *307*, 290–299.

Kodama, Y., Hijikata, M., Kageyama, R., Shimotohno, K., and Chiba, T. (2004). The role of notch signaling in the development of intrahepatic bile ducts. Gastroenterology *127*, 1775–1786.

Lebrun, G., Vasiliu, V., Bellanne-Chantelot, C., Bensman, A., Ulinski, T., Chretien, Y., and Grunfeld, J. P. (2005). Cystic kidney disease, chromophobe renal cell carcinoma and TCF2 (HNF1 beta) mutations. Nat. Clin. Pract. Nephrol. *1*, 115–119.

Lemaigre, F. P. (2003). Development of the biliary tract. Mech. Dev. *120*, 81–87.

Liu, J., Nethery, D., and Kern, J. A. (2004). Neuregulin-1 induces branching morphogenesis in the developing lung through a P13K signal pathway. Experimental lung Res. *30*, 465–478.

Low, Y., Vijayan, V., and Tan, C. E. (2001). The prognostic value of ductal plate malformation and other histologic parameters in biliary atresia: an immunohistochemical study. J. Pediatr.*139*, 320–322.

Lubarsky, B., and Krasnow, M. A. (2003). Tube morphogenesis: making and shaping biological tubes. Cell *112*, 19–28.

Martin-Belmonte, F., Gassama, A., Datta, A., Yu, W., Rescher, U., Gerke, V., and Mostov, K. (2007). PTEN-mediated apical segregation of phosphoinositides controls epithelial morphogenesis through Cdc42. Cell *128*, 383–397.

McCright, B., Lozier, J., and Gridley, T. (2002). A mouse model of Alagille syndrome: Notch2 as a genetic modifier of Jag1 haploinsufficiency. Development *129*, 1075–1082.

O'Brien, L. E., Yu, W., Tang, K., Jou, T. S., Zegers, M. M., and Mostov, K. E. (2006). Morphological and biochemical analysis of Rac1 in three-dimensional epithelial cell cultures. Methods Enzymol. *406*, 676–691.

Ojakian, G. K., Ratcliffe, D. R., and Schwimmer, R. (2001). Integrin regulation of cell-cell adhesion during epithelial tubule formation. J. Cell Sci. *114*, 941–952.

Ojakian, G. K., and Schwimmer, R. (1994). Regulation of epithelial cell surface polarity reversal by beta 1 integrins. J. Cell Sci. *107*(Pt 3), 561–576.

Paumgartner, G. (2006). Medical treatment of cholestatic liver diseases: From pathobiology to pharmacological targets. World J. Gastroenterol. *12*, 4445–4451.

Schmucker, D. L., Ohta, M., Kanai, S., Sato, Y., and Kitani, K. (1990). Hepatic injury induced by bile salts: correlation between biochemical and morphological events. Hepatology *12*, 1216–1221.

Sergi, C., Adam, S., Kahl, P., and Otto, H. F. (2000). Study of the malformation of ductal plate of the liver in Meckel syndrome and review of other syndromes presenting with this anomaly. Pediatr. Dev. Pathol. *3*, 568–583.

Tan, C. E., Chan, V. S., Yong, R. Y., Vijayan, V., Tan, W. L., Fook Chong, S. M., Ho, J. M., and Cheng, H. H. (1995). Distortion in TGF beta 1 peptide immunolocalization in biliary atresia: comparison with the normal pattern in the developing human intrahepatic bile duct system. Pathol. Int. *45*, 815–824.

Tang, M. J., Cai, Y., Tsai, S. J., Wang, Y. K., and Dressler, G. R. (2002). Ureteric bud outgrowth in response to RET activation is mediated by phosphatidylinositol 3-kinase. Dev. Biol. *243*, 128–136.

Tanimizu, N., and Miyajima, A. (2004). Notch signaling controls hepatoblast differentiation by altering the expression of liver-enriched transcription factors. J. Cell Sci. *117*, 3165–3174.

Tanimizu, N., Miyajima, A., and Mostov, K. E. (2007). Liver progenitor cells develop cholangiocyte-type epithelial polarity in three-dimensional culture. Mol. Biol. Cell *18*, 1472–1479.

Tanimizu, N., Nishikawa, M., Saito, H., Tsujimura, T., and Miyajima, A. (2003). Isolation of hepatoblasts based on the expression of Dlk/Pref-1. J. Cell Sci. *116*, 1775–1786.

Tanimizu, N., Saito, H., Mostov, K., and Miyajima, A. (2004). Long-term culture of hepatic progenitors derived from mouse Dlk+ hepatoblasts. J. Cell Sci. *117*, 6425–6434.

Terada, T., and Nakanuma, Y. (1995). Detection of apoptosis and expression of apoptosis-related proteins during human intrahepatic bile duct development. Am. J. Pathol. *146*, 67–74.

Walid, S., Eisen, R., Ratcliffe, D. R., Dai, K., Hussain, M. M., and Ojakian, G. K. (2008). The PI 3-kinase and mTOR signaling pathways are important modulators of epithelial tubule formation. J. Cell. Physiol. *216*, 469–479.

Weiner, O. D., Neilsen, P. O., Prestwich, G. D., Kirschner, M. W., Cantley, L. C., and Bourne, H. R. (2002). A PtdInsP(3)- and Rho GTPase-mediated positive feedback loop regulates neutrophil polarity. Nat. Cell Biol. *4*, 509–513.

Yoon, J. H., and Gores, G. J. (2002). Death receptor-mediated apoptosis and the liver. J. Hepatol. *37*, 400–410.

Yu, W., O'Brien, L. E., Wang, F., Bourne, H., Mostov, K. E., and Zegers, M. M. (2003). Hepatocyte growth factor switches orientation of polarity and mode of movement during morphogenesis of multicellular epithelial structures. Mol. Biol. Cell *14*, 748–763.

Zegers, M. M., O'Brien, L. E., Yu, W., Datta, A., and Mostov, K. E. (2003). Epithelial polarity and tubulogenesis in vitro. Trends Cell Biol. *13*, 169–176.

Zohn, I. E., Chesnutt, C. R., and Niswander, L. (2003). Cell polarity pathways converge and extend to regulate neural tube closure. Trends Cell Biol. *13*, 451–454.

Zuk, A., and Matlin, K. S. (1996). Apical beta 1 integrin in polarized MDCK cells mediates tubulocyst formation in response to type I collagen overlay. J. Cell Sci. *109*(Pt 7), 1875–1889.